

Facile Synthesis of Biomimetic Honeycomb Material with Biological Functionality

Jingyun Ma, Yu Sanna Hui, Min Zhang, Yue Yu, Weijia Wen, and Jianhua Qin*

Honeycomb in nature is constructed by bees for storing honey, larvae and pollen, exhibiting a delicate structure consisted of small hexagonal cells.^[1] In contrast to most insects and birds, bees construct their nests from their own secretions, revealing an important clue in the recognition of nest-mates and the understanding of the evolution of honeybee.^[1] The honeycomb structure has the most close packing geometry that allows the minimization of material for achieving light weight and low material cost, while provides minimal density, relatively high out-of-plane compression properties and in-plane elastic properties.^[2,3] Mimicking the honeycomb structure in nature will inspire us to develop novel composite materials for different applications, such as in aircraft design, motor vehicle technology and light-weight construction in aerospace.^[4–8]

Currently, honeycomb structure can be manufactured using a variety of materials, depending on the intended applications and design requirements, from paper or polymer^[9,10] with low strength/stiffness to aluminium, ceramics or glass fiber reinforced plastics^[11–13] with high strength/stiffness. Honeycomb composites have been used in different industries such as aerospace, environmental catalyst, packaging and electronics.^[8,14–16] Several methods have been reported to fabricate honeycomb structure including self-assembly, moulding-based extrusion and photolithography.^[17–22] However, these methods require complicated procedure and the formation of a biomimetic honeycomb structure still remains a challenge. Particularly, their implications as biological functionalized material are yet to be explored.

Poly (lactic-co-glycolic acid) (PLGA) is a type of copolymer with excellent biodegradability and biocompatibility.^[23,24] In particular, PLGA has been extensively studied in the development of devices for controlled delivery of small molecules, drugs, proteins and other macromolecules in commercial and research applications.^[23] Herein, we present a

novel and straightforward approach to synthesize biomimetic and multiscale honeycomb structure utilizing the synergistic effect of PLGA polymer precipitation, double emulsion template and internal effervescent salt decomposition. Compared to the conventional porous PLGA micro/nanoparticles, the resultant honeycomb structure exhibits unique characteristics including external nanoporous membrane and internal cavities, especially, with the most closely packing geometry that allows the minimization of material for achieving light weight and low material cost, while provides sufficient mechanical strength. All these properties are well mimicking the honeycomb structure in nature. Such biomimetic structure can be used as functional microcarriers in cell culture and drug delivery. The approach is very simple, facile, biocompatible and can be functionalized easily, therefore exhibiting powerful potentials in the areas of biology, tissue engineering and catalysis.

Prior to the experiment, a polydimethylsiloxane (PDMS) microfluidic device designed with flow-focusing structure was used to generate double emulsions by shearing primary emulsion phase with continuous aqueous phase. The local schematic diagram of the device was depicted in **Figure 1**. The double emulsions were composed of W_1 aqueous phase dissolving NH_4HCO_3 (inner phase), oil dissolving PLGA (middle phase) and W_2 poly(vinyl alcohol) (PVA) solution (external phase). The primary W_1/O emulsion was obtained from ultrasonic emulsification, in which W_1 phase was dispersed in oil phase. The primary emulsion was sheared by W_2 continuous phase into $W_1/O/W_2$ micro-droplets at the flow-focusing junction. The microfluidic channels were modified by poly(vinyl alcohol)/glycerol (PVA/Gly) in order to form hydrophilic surface for the $W_1/O/W_2$ droplets generation and movement without adhesion to the wall.^[25] As shown in Figure 1, once the $W_1/O/W_2$ double emulsions were formed, the interfacial oil evaporation resulted in the formation of a thin nanoporous membrane from the dissolved PLGA precipitation. Subsequently, rapid and heavy oil evaporation appeared from the interface to the interior led to the formation of PLGA precipitation around W_1 droplets. As the volume of the oil phase decreased, the distance between W_1 droplets decreased, causing W_1 droplets to extrude reciprocally, and thus deforming W_1 droplets from circular to honeycomb-like hexagonal shape. Meanwhile, the decomposition reaction of effervescent NH_4HCO_3 in W_1 droplets occurred due to the contact of W_1 and W_2 , which generated carbon dioxide and ammonia to disperse W_1 droplets and protected

J. Y. Ma, M. Zhang, Y. Yu, Prof. J. H. Qin
Dalian Institute of Chemical Physics
CAS, Dalian 116023, PR China
E-mail: jhqin@dicp.ac.cn

Y. S. Hui, Dr. Prof. W. J. Wen
Department of Physics
The Hong Kong University of Science and Technology
Clear Water Bay, Kowloon, Hong Kong



DOI: 10.1002/sml.201201624

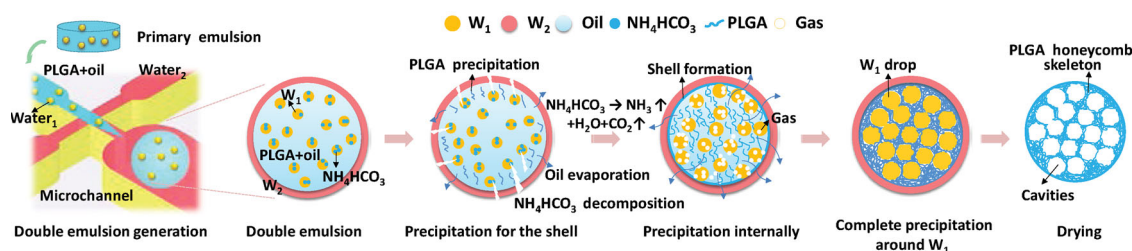


Figure 1. Schematic diagram of the formation process of the honeycomb structure microspheres.

them from coalescence.^[26] Individual W_1 droplets and the surrounding gas bubbles occupied the internal space of the microsphere and resulted in hollow multiple cavities after PLGA precipitation and water phase removal.

In this work, it was noted that the dimethyl carbonate solvent in oil phase played a key role in the formation of the unique honeycomb structure for biological applications. Different from the solvent (CH_2Cl_2) commonly used for preparing PLGA matrix, the organic dimethyl carbonate we used had favorable properties including rapid evaporation, non-swelling against PDMS, non-toxicity and biocompatibility.^[27] Particularly, the rapid evaporation attribute of dimethyl carbonate not only promoted the prior membrane formation outside of the microspheres, but also facilitated the PLGA solidification only within 1 min, in contrary to 3–4 h using CH_2Cl_2 .^[26]

To ensure complete solidification of PLGA microspheres without coalescence before entering the reservoir, several parameters such as the fluid flow rate and channel geometry should be optimized according to the volume shrink proportion and solidification rate of the $W_1/O/W_2$ double emulsion. Under optimized experimental conditions, stable and mono-disperse micro-droplets with suitable sizes could be continuously generated and solidified into PLGA microspheres (when the flow rates of W_1/O and W_2 phases were $0.5 \mu\text{L}/\text{min}$ and $8 \mu\text{L}/\text{min}$, respectively, and the width/height of the flow-focusing structure were fixed at $100 \mu\text{m}$).

During the experiment, we found that NH_4HCO_3 concentration had predominant influence on the diameters of the honeycomb microspheres. Figure 2a–c depicted the images of microspheres prepared with different concentrations of NH_4HCO_3 porogen in W_1 . With increasing amount

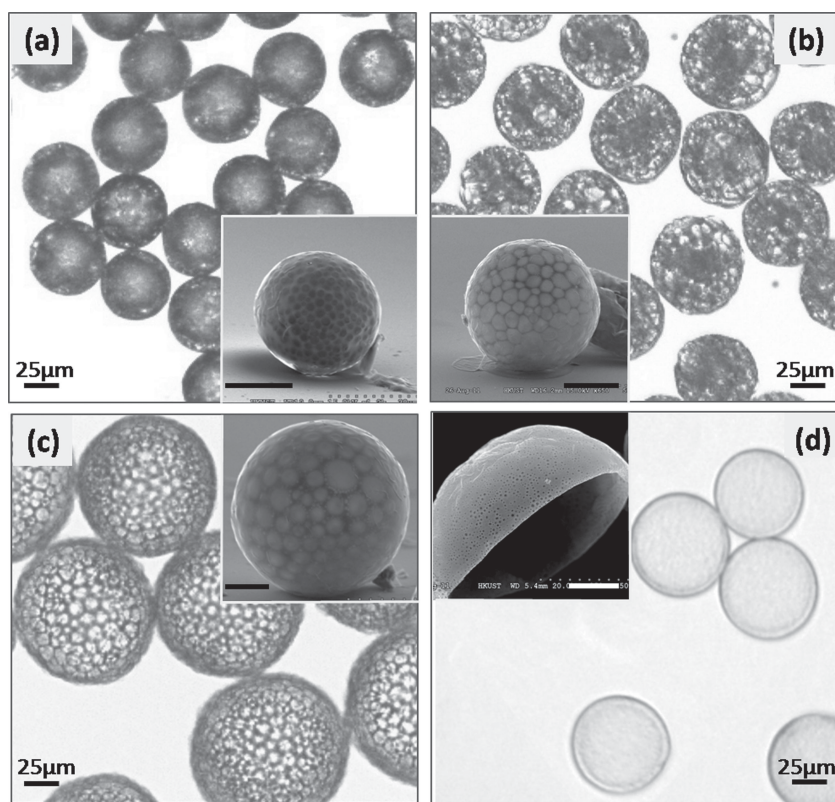


Figure 2. (a–c) Optical images of the honeycomb structure PLGA microspheres prepared with primary emulsion containing 1%, 5% and 10% NH_4HCO_3 in W_1 phase, respectively. The primary emulsion was placed for 72 h after ultrasonic emulsification. (d) The formation of hollow structure PLGA microspheres prepared with primary emulsion containing 10% NH_4HCO_3 after immediate ultrasonic emulsification. Insets: SEM images of corresponding microsphere in (a–d).

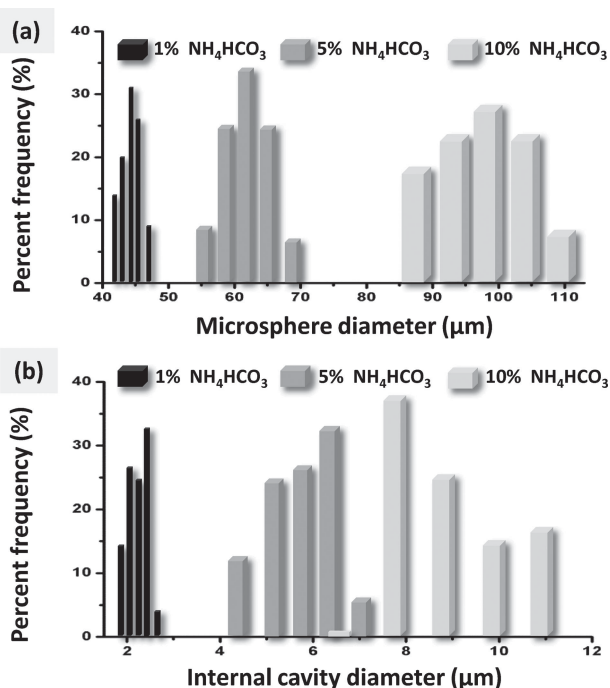


Figure 3. (a) Size distributions of the honeycomb structure PLGA microspheres, $n = 100$. (b) Size distributions of internal cavities inside the microspheres, $n = 50$. In each graph, data series from left to right represent NH_4HCO_3 concentration at 1%, 5%, and 10% in the W_1 phase.

of NH_4HCO_3 , no discernible difference in morphology was observed. However, the increase in NH_4HCO_3 concentration was closely related to the diameters of microspheres and the sizes of internal cavities within the microspheres, as illustrated in **Figure 3**. Under different concentrations of NH_4HCO_3 (1%, 5% and 10%), the average diameters of microspheres were 44.67 μm, 61.93 μm and 97.61 μm, while the average sizes of internal cavities within the microspheres were 2.28 μm, 5.79 μm and 8.70 μm, respectively. The main reason for such relationship was that the internal gas formation expanded the W_1 aqueous droplets. Meanwhile, the gas bubbles escaping from W_1 phase into oil phase increased the volume of PLGA skeleton. Together, these two factors generated larger microspheres with higher NH_4HCO_3 concentration, whilst more gas contributed to larger internal cavities.

The variation coefficients of the fabricated PLGA microspheres were further investigated. Under different NH_4HCO_3 concentrations (from 1% to 10%), the variation coefficients of the PLGA microsphere diameters were 3.40%, 5.77% and 7.01%, suggesting that the diameter distribution of resultant microspheres was widened with the increasing amount of NH_4HCO_3 , in which the microspheres with

1% NH_4HCO_3 exhibited the sharpest distribution. In fact, as more gas bubbles formed in the $W_1/O/W_2$ double emulsion, the internal microenvironment appeared at a higher chaotic state, thus influencing the monodispersity of microspheres. As shown in SEM images in **Figure 2a-c**, the tiny cavities surrounding the larger micro-cavities were clearly visible. It was assumed that these tiny cavities were mainly generated from the gas bubbles which played an important role in preventing W_1 droplets from coalescence. In addition, we observed that the long term placement of the primary emulsion was critical for defining the formation and morphology of the honeycomb structure as shown in **Figure 2a-c**. Otherwise, only PLGA microspheres with hollow structure were generated if primary emulsion was used immediately after ultrasonic emulsification, as illustrated in **Figure 2d**.

In order to characterize the biomimetic honeycomb structure, the fluorescence dye Rhodamine-123 (Rh-123) was incorporated into W_1 phase to illustrate the distribution of membrane and internal cavities of the PLGA microspheres as depicted in **Figure 4**. As a result of the strong adsorption effect of Rh-123 onto PLGA and the removal of W_1 phase, the entire PLGA skeleton including the external membrane and the edges of the internal cavities emitted green fluorescence. As shown in the inset of **Figure 4**, the internal scaffold structure wrapped by the outer membrane was clearly visible and the inner micro-cavities appeared as hexagonal or circular in shape, resembling the unit cell of a honeycomb.

Based on the above synthesis method, the material exhibited unique honeycomb structure with internal micro-cavities

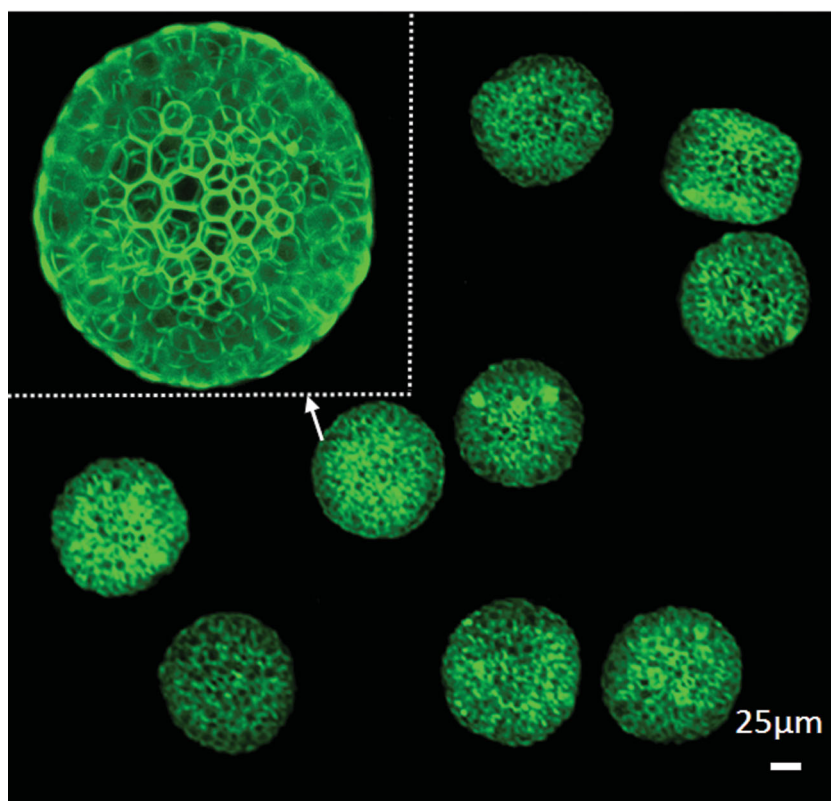


Figure 4. Confocal fluorescence projection images (Z axis) of the synthesized microsphere.

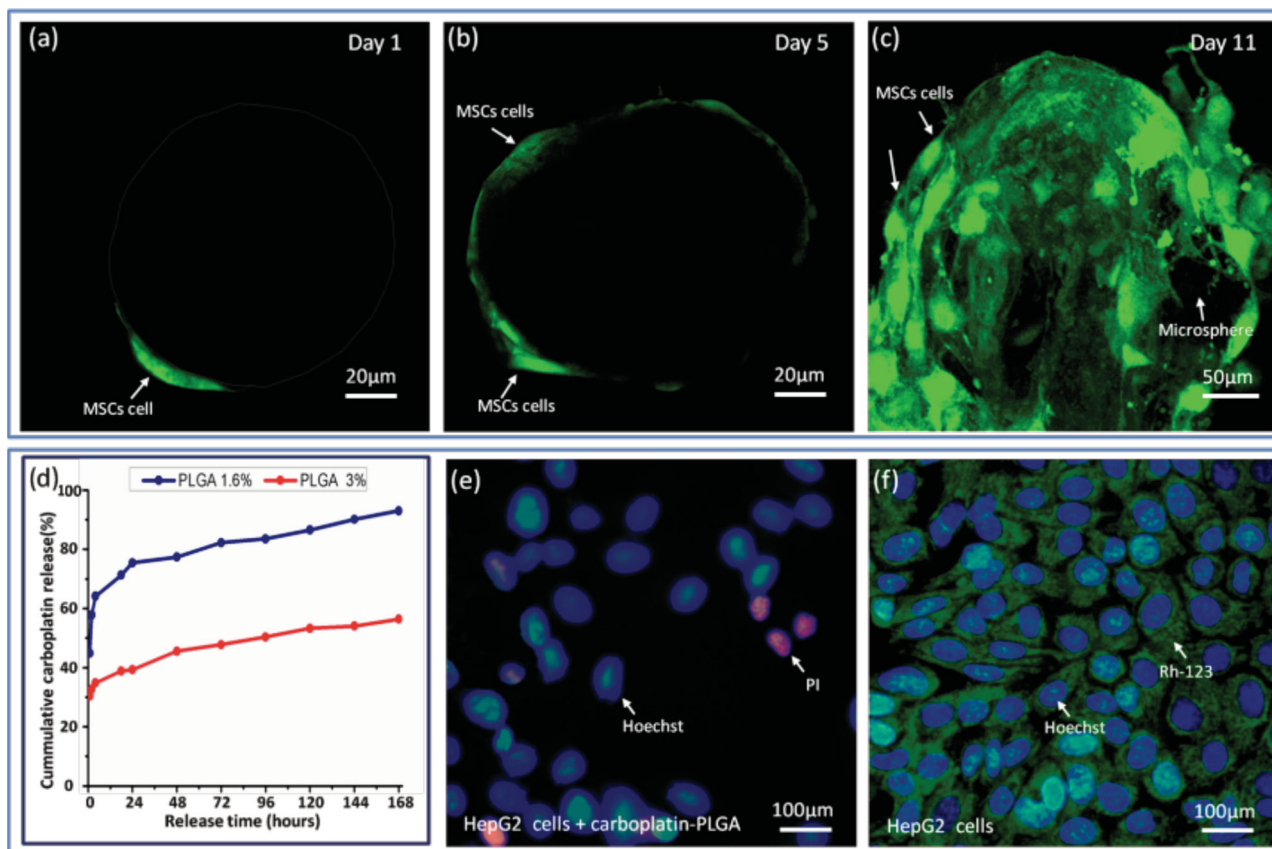


Figure 5. Exploration of the biological functions of the honeycomb structure as microcarriers for cell culture and drug release. (a-c) Proliferation of MSCs (transfected with GFP gene) on the surface of honeycomb microspheres after culturing for 1 day, 5 days and 11 days. (d) Drug releasing profiles of carboplatin-loaded microspheres with PLGA concentration at 1.6% and 3% in preparation, respectively. (e-f) Chemosensitivity test of carboplatin-PLGA microspheres on the cytotoxicity of HepG2 cells. (e) Fluorescence images of HepG2 cells exposed to carboplatin-PLGA for 3 days. (f) Fluorescence images of control group.

surrounded by external nanoporous membrane. In terms of the non-toxic and biocompatible synthesis system, such biomimetic microspheres embraced themselves with obvious advantages, such as the higher membrane permeability and biocompatibility. Particularly, the internal cavities allowed encapsulation and selective release of substance such as particles, drug and gas, which might be desirable for bio-applications.

Initially, we explored the capability of honeycomb structure as a microcarrier for stem cell culture. Bone marrow derived mesenchymal stem cells (MSCs) in medium suspension were co-cultured with microspheres for different days, then the MSCs were observed using confocal laser scanning microscope. As shown in **Figure 5a-b**, MSCs that were immobilized on the microsphere surface exhibited good adhesion property after cultivating for 1 day, progressive proliferation was demonstrated after 5 days which indicated the microspheres had provided a good environment for culturing cells. Most importantly, the unique honeycomb structure of the microspheres incorporating with nanoporous membrane and internal cavities could offer continuous flow of nutrients and oxygen that were essential for cell growth. The porosity of the structure could potentially provide enhancement for colonization in tissue

engineering. In the following experiment, it was observed that the cells attached to the microspheres could aggregate gradually after long culturing time and formed a colony of “tiny tissue” as shown in **Figure 5c**, and this should be useful for the formation of complex in-vivo growth of tissue or organ. During this successive culture process, we tested the cell viability of the aggregate by PI staining. The cells exhibited good viability after 11 days culture without dead cells observed, indicating the compatible property of this structure as micro-carrier for cell culture. The good biological function for cell culture was mainly due to the sufficient capacity for nutrients and oxygen exchange offered by the honeycomb microspheres. Particularly, the cells immobilized on the microsphere could also be protected from the shear stress, accompanying with the sufficient diffusion of oxygen and nutrients.

In most cases, such kind of micro-carrier culture was accommodated with higher surface-to-volume ratio and higher cell densities than those obtained in static dish culturing. The area available for cell growth could be adjusted easily by changing the amount of micro-carriers, thus simplifying scale-up process. From commercial or clinical points of view, this quantization feature had a tremendous impact owing to the less cost in cell manufacturing by reducing the

amount of media, growth factors and other expensive supplements required in stem cell cultivation.

In addition to cell micro-carriers, the honeycomb structure material was further investigated to encapsulate molecular compound in drug release. Carboplatin is a widely used anti-cancer drug for systemic administrations. To explore the honeycomb microspheres as microcarriers in drug release, hydrophilic carboplatin was encapsulated in the microspheres during the formation of double emulsions. As shown in Figure 5d, the results plotted the kinetic profiles of in-vitro release of carboplatin from drug-loaded PLGA microspheres. The results were expressed as the percentage of carboplatin released versus time. In this graph, two distinctive kinetic profiles could be clearly identified. Microspheres with 1.6% PLGA resulted in a kinetic profile of carboplatin release with a sharper initial burst than those microspheres with 3% PLGA. The initial burst was probably due to the fact that the absorbed carboplatin at the surface of the microspheres was dissolved into aqueous phase, followed by the diffusion and degradation dominating the subsequent drug release process. We found that the microspheres with 3% PLGA exhibited a denser membrane structure and a slower degradation rate than those with lower concentration of PLGA (1.6%).

We further performed the chemosensitivity test of carboplatin-loaded microcarriers for drug release in human hepatocellular carcinoma (HepG2) cells. Three kinds of fluorescent dyes were used as indicators to evaluate cell growth inhibition and apoptosis triggered by carboplatin released from the microcarriers. Comparing with the HepG2 cells cultured alone in Figure 5f, the cells exposed to carboplatin-loaded microcarriers exhibited distinctive differences in terms of morphology, nuclear condensation, and plasma membrane permeability (Figure 5e). Carboplatin-loaded PLGA structure exhibited obvious growth inhibition and apoptosis effect on HepG2 cells after exposure to cells for 3 days. The cell apoptosis was characterized by the reduced green fluorescence signal (Rh-123, mitochondrial transmembrane potential), the increase in blue fluorescence condensation (Hoechst 33342, nuclear condensation) as well as red fluorescence (PI, plasma membrane permeability increased). The results indicated that these carboplatin-loaded microspheres had the ability to suppress tumor activity by inhibiting of proliferation and inducing apoptosis in HepG2 cells. These drug-loaded honeycomb microspheres may offer a moderate manner for drug release as compared to the cells exposed to carboplatin alone. It is noted that, the honeycomb microspheres can exhibit multiple functionalities for drug release, which can encapsulate and release not only hydrophilic compounds, but also hydrophobic compounds as well, which is not possible by conventional porous PLGA micro/nanoparticles, and this is expected to offer attractive attributes for serving as micro-carriers in drug delivery.

In summary, this study successfully demonstrated a novel and straightforward approach for biomimetic synthesis of delicate honeycomb structure with biological functions. The synergistic effect of PLGA rapid precipitation, double emulsion template and effervescent salt decomposition resulted in the formation of unique honeycomb structure, which was

not possible by other methods. By varying the concentration of the effervescent agent, the size of the honeycomb structure and internal cavities can be tuned flexibly. The biological functions of the honeycomb structure were demonstrated by serving as micro-carriers for cell culture and drug release as well. The synthesis method offered obvious advantages such as simplicity, good biocompatibility and functionality, revealing its powerful potentials for applications in drug delivery, tissue engineering, and even some implications in catalysis field.

Experimental Section

Reagents: Poly(lactic-co-glycolic acid) (PLGA, viscosity 1.64 dL/g) was purchased from Changchun SinoBiomaterials Co., Ltd. Carboplatin was bought from Qilu Pharmaceutical Co., Ltd. Dimethyl carbonate and ammonium bicarbonate (NH_4HCO_3 , analytical-grade) were bought from Tianjing Chemical Reagent Research Institute. Polydimethylsiloxane (PDMS) (Sylgard 184) was purchased from Dow Corning Company. SU-8 (3035) photoresist was purchased from MicroChem. Poly (vinyl alcohol)(PVA, 1750 \pm 50) was purchased from Tianjin Fuchen Chemical Reagent. Glycerol (Gly) was purchased from Tianjin Nankai Chemical Factory. Rhodamine 123 (Rh-123, Sigma Chemicals Co., St. Louis, MO. USA) was used as the fluorescence indicator for the characterization of PLGA microspheres. This Rh-123 and Hoechst 33342 (Molecular Probes, Eugene, OR, USA), propidium iodide (PI, Molecular Probes, Eugene, OR, USA) were used for the fluorescence probes to identify cell activity. All reagents were analytical-grade or better. α -MEM (minimum essential medium, Sigma) with 10% fetal bovineserum (HyClone) was used for marrow stromal cell culture. High-glucose medium (DMEM, Sigma) with 10% fetal bovine serum (HyClone) was used for HepG2 cell culture. Solutions were prepared with deionized (DI) water unless otherwise specified.

Instruments: Ultrasonic crusher JY92-IIN (Ningbo Scientz Biotechnology Co.Ltd.) was used for ultrasonic emulsification of the primary emulsion. Bright field and fluorescence observations were carried out using an inverted fluorescence microscope (Olympus IX71, Japan) equipped with a CCD camera (MicroPublisher RTV 5.0, QImaging). Scanning Electron Microscopy (provided by HKUST) was used to study the morphology of the specimens. Confocal Laser Scanning Biological Microscope (Olympus FV1000, Japan) was used for three-dimensional reconstructions of the objects. LC-20AD UFLC (Shimazu, Japan) system coupled with a SPD-20A UV/VIS detector (Shimazu, Japan) was used to analyze the released carboplatin concentrations. Syringe pumps (Longerpump, L0107-1A, Hebei, China) were used to deliver different phases to the micro-fluidic device. Water-bathing constant temperature vibrator (THZ-82, Jintan Huafeng instrument Co., Ltd.) was used in the drug releasing process. High speed micro-centrifuge (TG16-W) was used for purifying the resultant solutions.

Design, Fabrication, and Modification of the Microfluidic Device: A positive mold patterned from photoresist SU-8 3035 using standard soft lithography procedure was used to fabricate PDMS substrate containing microchannels. After punching, plasma treatment and sealing, the integrated microfluidic device was formed as depicted in Figure 1. The device consisted of a flow-focusing structure for droplet generation with channel width of

100 μm and height of 100 μm , a collection channel in the downstream with width of 250 μm and height of 218 μm .

Immediately after oxygen plasma treatment of the PDMS and glass slide, a drop of poly (vinyl alcohol)/glycerol (PVA/Gly, 2/5 wt%) aqueous solution was added to the outlet reservoir at the end of the microchannel. Due to surface tension, PVA/Gly solution flooded the entire microchannel spontaneously. After 20 min, the vacuum was applied to the PDMS device to remove excess PVA/Gly solution. The device was then placed in an oven at 60 °C for 2 h to consolidate the adsorption of PVA/Gly to the channel surface. The entire process was repeated once. Finally, the device was subject to 20 min at 100 °C followed by natural cooling.

Synthesis and Characterization of PLGA Microspheres: Preparation of primary W_1/O emulsion: 0.3 mL freshly-prepared NH_4HCO_3 solution (1%, 5%, and 10%, wt%) was mixed with the oil phase of dimethyl carbonate containing PLGA (1.6%) at 3:10 volume ratio. Ultrasonic crusher was used for emulsification at 40 W for 5 s in an ice bath, then the emulsion stood for a period of 72 h.

Preparation of PLGA microspheres: Syringe pumps were used to deliver the primary W_1/O emulsion and continuous phase W_2 to the microfluidic device. The continuous phase W_2 consisted of DI water containing PVA (2 wt%) as the surfactant. Primary W_1/O emulsion obtained from ultrasonic emulsification was sheared into $W_1/O/W_2$ micro-droplets at the flow-focusing structure in the microfluidic device. By adjusting the flow rates of W_1/O and W_2 phases, micro-droplets with different sizes and solidification time were formed in the channel and collected at the outlet reservoir to a storage bottle using a pipette. The resultant microspheres were washed 3 times with DI water and vacuum-dried overnight.

Fluorescence and SEM characterization of PLGA microspheres: Rhodamine 123 (5×10^{-6} g/mL in W_1) was used as the fluorescence indicator for characterizing dried PLGA microspheres with 10% NH_4HCO_3 . Specimen preparation for SEM involved drying a drop of dispersion on a glass slide using a vacuum oven followed by the sputtering of a thin gold layer. The spatial parameters including the microsphere diameter ($n = 100$) and inner cavity sizes ($n = 50$) were determined by an image analysis software Image-Pro (Media Cybernetics) based on the optical and SEM photographs of the resultant PLGA microspheres prepared with different concentrations of NH_4HCO_3 porogen in W_1 (1%, 5% and 10%).

Evaluation of the Microspheres as Cell Microcarriers: Marrow stromal cells (MSCs) were isolated from mouse bone marrow and transfected with the green fluorescent protein gene. The cells were cultured in α -MEM with 10% fetal bovine serum containing penicillin (100 U/mL) and streptomycin (100 $\mu\text{g}/\text{mL}$). To investigate the cell proliferation on PLGA microspheres, matrices with NH_4HCO_3 concentration at 10% were sterilized by soaking them in ethanol overnight. The ethanol was then replaced with phosphate buffered saline (PBS, pH 7.4) followed by α -MEM. Drops of medium suspension containing MSCs ($\sim 10^3$ cells/mL) and PLGA microspheres ($\sim 10^3/\text{mL}$) were dripped on the petri dish cover, faced downward and placed in the incubator for culture. The matrices with MSCs were cultured for different period of times (1 day, 5 days, 11 days) and evaluated using confocal laser scanning microscope.

Evaluation of the Microspheres as Drug Microcarriers: 0.15 mL carboplatin solution was mixed with the oil phase of dimethyl carbonate containing PLGA (1.6% or 3%) at 3:20 volume ratio.

Ultrasonic crusher was used for the ultrasonic emulsification of the mixture at 40 W for 5 s in an ice bath. 0.15 mL freshly prepared NH_4HCO_3 solution (2%, wt%) was added to the above emulsion and subject to the same ultrasonic conditions. Other processing steps were the same as those described in the preparation of PLGA microspheres. PLGA microspheres loaded with carboplatin and 1% NH_4HCO_3 were collected at low flow rates of 8 $\mu\text{L}/\text{min}$ (W_2 phase) and 0.5 $\mu\text{L}/\text{min}$ (W_1/O phase) respectively for 2 h. Microspheres were then washed to remove PVA and suspended in phosphate buffered saline (PBS, pH 7.4) with the final fixed volume of 2 mL. The microspheres were then subject to constant vibration at 100 rpm (37 °C) in a glass bottle. Samples at different time scales (1 h, 2 h, 4 h, 18 h, 24 h, 48 h, 3 days, 4 days..., 8 days) were subject to centrifugation at 3000 rpm for 5 min to isolate microspheres from the suspension. 1 mL of the supernatant was used for analysis and an equal volume of fresh PBS solution was added to the remaining solution. Carboplatin concentrations were analyzed by LC-20AD UFLC (Shimadzu, Japan) system with a 4.6 mm \times 250 mm, 5 μm reverse-phase Symmetry C18 column (Waters, Ireland), coupled to a SPD-20A UV/VIS detector (Shimadzu, Japan) at 230 nm absorptive wavelength. The separation condition was at 40 °C with a mobile phase of methanol/water (15/85, v/v) at a flow rate of 0.5 mL/min for 10 min. After 8 days, the suspension was centrifuged to isolate microspheres from the solution, and then the microspheres were dried and dissolved in dimethyl carbonate. DI water was added to the dimethyl carbonate solution followed by shaking to allow carboplatin extraction. The resultant mixture experienced phase separation for 30 min before subjecting to carboplatin measurement. Standard UV absorbance curve of carboplatin at 230 nm was obtained with concentration ranging from 0.1 $\mu\text{g}/\text{mL}$ to 20 $\mu\text{g}/\text{mL}$ ($r^2 \approx 0.999$). The percentage of carboplatin released at each time scale was calculated by normalizing the data collected with the cumulative amount of released carboplatin contained in the PLGA microspheres. The kinetic profiles of drug release represented the average data of triplicate independent experiments in parallel.

HepG2 cells were cultured in a high-glucose medium with 10% fetal bovine serum containing penicillin (100 U/mL) and streptomycin (100 $\mu\text{g}/\text{mL}$). For chemosensitivity test, HepG2 cells were cultured in a growth medium with carboplatin-PLGA microspheres (PLGA concentration at 3%) for 3 days. After in-vitro drug exposure, HepG2 cells were labeled with the fluorescent dyes (Rh-123, Hoechst 33342 and PI) for characterization. Using an inverted fluorescence microscope, the fluorescent images were captured and the change of apoptosis markers, including MMP, nuclear morphology and plasma membrane permeability were analyzed accordingly.

Acknowledgements

This research was supported by the Joint Research Fund of NSFC-RGC (11161160522, N_HKUST601/11), Knowledge Innovation Program of the Chinese Academy of Sciences (KJCX2-YW-H18), and Instrument Research and Development Program of the Chinese Academy of Sciences (YZ200908).

- [1] K. Zhang, H. L. Duan, B. L. Karihaloo, J. X. Wang, *Proc. Natl. Acad. Sci. USA* **2010**, *107*, 9502.
- [2] F. Côté, B. P. Russell, V. S. Deshpande, N. A. Fleck, *J. Appl. Mech.* **2009**, *76*, 061004.
- [3] C. M. Taylor, C. W. Smith, W. Miller, K. E. Evans, *Int. J. Solids Struct.* **2011**, *48*, 1330.
- [4] U. H. F. Bunz, *Adv. Mater.* **2006**, *18*, 973.
- [5] B. Xu, F. Arias, G. M. Whitesides, *Adv. Mater.* **1999**, *11*, 492.
- [6] J. K. Paik, A. K. Thayamballi, G. S. Kim, *Thin-Walled Struct.* **1999**, *35*, 205.
- [7] H. Zhao, G. Gary, *Int. J. Impact Engng.* **1998**, *21*, 827.
- [8] U. Martin, D. Ehinger, L. Kruger, S. Martin, T. Mottitschka, C. Weigelt, C. G. Aneziris, M. Herrmann, *Adv. Mater. Sci. Eng.* **2010**, 269537.
- [9] C. C. Foo, G. B. Chai, L. K. Seah, *Compos. Struct.* **2007**, *80*, 588.
- [10] E. Min, K. H. Wong, M. H. Stenzel, *Adv. Mater.* **2008**, *20*, 3550.
- [11] H. N. G. Wadley, N. A. Fleck, A. G. Evans, *Compos. Sci. Technol.* **2003**, *63*, 2331.
- [12] X. C. Quan, H. C. Shi, Y. M. Zhang, J. L. Wang, Y. Qian, *Process. Biochem.* **2003**, *38*, 1545.
- [13] N. J. Lombardi, J. Liu, *Compos. Struct.* **2011**, *93*, 1275.
- [14] M. C. Carlos, F. P. C. Agustín, *Materials* **2010**, *3*, 1203.
- [15] Z. Y. Xue, J. W. Hutchinson, *Int. J. Numer. Meth. Engng.* **2006**, *65*, 2221.
- [16] J. Wang, H. X. Shen, C. F. Wang, S. Chen, *J. Mater. Chem.* **2012**, *22*, 4089.
- [17] S. A. Jenekhe, X. L. Chen, *Science* **1999**, *283*, 372.
- [18] L. A. Connal, G. G. Qiao, *Adv. Mater.* **2006**, *18*, 3024.
- [19] W. F. Bu, H. L. Li, H. Sun, S. Y. Yin, L. X. Wu, *J. Am. Chem. Soc.* **2005**, *127*, 8016.
- [20] R. Yang, T. N. Chen, H. L. Chen, W. J. Wang, *Sens. Actuators, B* **2005**, *106*, 506.
- [21] J. H. Kim, M. Seo, S. Y. Kim, *Adv. Mater.* **2009**, *21*, 4130.
- [22] G. C. Engelmayr, M. Y. Cheng, C. J. Bettinger, J. T. Borenstein, R. Langer, L. E. Freed, *Nat. Mater.* **2008**, *7*, 1003.
- [23] R. A. Jain, *Biomaterials* **2000**, *21*, 2475.
- [24] S. W. Choi, Y. C. Yeh, Y. Zhang, H. W. Sung, Y. N. Xia, *Small* **2010**, *6*, 1492.
- [25] T. X. He, Q. L. Liang, K. Zhang, X. Mu, T. T. Luo, Y. M. Wang, G. A. Luo, *Microfluid. Nanofluid.* **2011**, *10*, 1289.
- [26] T. K. Kim, J. J. Yoon, D. S. Lee, T. G. Park, *Biomaterials* **2006**, *27*, 152.
- [27] F. Aricò, P. Tundo, *Russ. Chem. Rev.* **2010**, *79*, 479.

Received: July 10, 2012
Revised: September 10, 2012
Published online: